Contribution from the Departments of Chemistry, Florida Atlantic University, Boca Raton, Florida 33431, Purdue University School of Science, Indiana University-Purdue University at Indianapolis, Indianapolis, Indiana 46223, and Notre Dame University, Notre Dame, Indiana 46556

Synthesis, Electrochemistry, and Spectroscopic Properties of Six-Coordinate Monooxomolybdenum(VI) Complexes Containing Tridentate Schiff Base and Bidentate Catecholate Ligands. Crystal and Molecular Structure of (*N*-Salicylidene-2-aminophenolato)(naphthalene-2,3-diolato)oxomolybdenum(VI)

Jalal U. Mondal,[1a] Franklin A. Schultz,*,[1b] Theodore D. Brennan,[1c] and W. Robert Scheidt*,[1c]

Received June 7, 1988

Six-coordinate monooxomolybdenum(VI) complexes, MoO(cat)(Sap), where Sap^{2-} = the Schiff base dianion *N*-salicylidene-2-aminophenolate and cat^{2-} = catecholate (Cat^{2-}), naphthalene-2,3-diolate ($Naphcat^{2-}$), or 3,5-di-*tert*-butylcatecholate ($DTBcat^{2-}$), are prepared by reacting the Mo(VI) dimer, $[MoO_2(Sap)]_2$, with the appropriate catechol. The products are characterized by cyclic voltammetry, mass spectrometry, and UV/vis, IR, and ^{95}Mo NMR spectroscopy. The MoO(cat)(Sap) complexes represent the first examples of a mononuclear MoO^{4+} center with a coordination number of six. The crystal structure of the MoO(Naphcat)(Sap) derivative is reported, confirming the six-coordinate, distorted octahedral environment about Mo(VI). Crystal data for MoO(Naphcat)(Sap): monoclinic, a = 9.961 (3) Å, b = 10.109 (2) Å, c = 38.929 (9) Å, β = 92.45 (2)°, V = 3916.4 Å^3, Z = 8, space group $P2_1/n$, 5863 unique observed data, R_1 = 0.081 and R_2 = 0.097, all observations at 292 K. There are two crystallographically independent molecules in the unit cell. The two complexes have an average Mo=O distance of 1.685 (17) Å, and Mo—O = 1.948 (15) Å and Mo—N = 2.259 (10) Å. The terminal oxo ligand and the central nitrogen donor of the *N*-salicylidene-2-aminophenolate ligand occupy opposite vertices of the octahedron; the four anionic oxygen donors of the bidentate and tridentate ligands define an equatorial plane. Bond angles in the coordination group deviate from the ideal value of 90° as a consequence of the ligand bite constraints and because all four O-Mo-O angles involving the terminal oxo ligand are larger than the ideal 90° value. MoO(cat)(Sap) complexes undergo reversible one-electron reduction at -0.5 to -0.7 V versus $Fc^{+/0}$ followed by irreversible one-electron reduction at -1.6 to -1.9 V. Reversible MoO^{4+}/MoO^{3+} electrochemistry is attributed to the fact that the Mo d_{xy} orbital of MoO(cat)(Sap) can be singly occupied upon reduction to Mo(V) without unfavorable interaction with the four bonds in its equatorial plane. This contrasts with the irreversible electrochemical behavior of seven-coordinate MoO^{4+} complexes, which contain five such bonds. The ^{95}Mo NMR chemical shift of MoO(Naphcat)(Sap) is +385 ppm versus external molybdate; this value is highly deshielded with respect to seven-coordinate MoO^{4+} and six-coordinate MoO_2^{2+} complexes with O and N donors.

Introduction

Oxomolybdenum chemistry is of interest because this functionality exists in several enzymes[2] and many catalytic systems.[3] The *cis*-dioxo moiety, MoO_2^{2+}, is the most commonly encountered structural form in Mo(VI) coordination chemistry.[2a] However, many complexes containing the monooxo Mo(VI) center, MoO^{4+}, have been prepared.[4-10] The latter compounds typically exhibit seven-coordinate, pentagonal-bipyramidal geometry.[4,6-8] We have examined the electrochemistry of a number of these complexes.[10,11]

Recently, we reported the preparation and preliminary electrochemical investigation of three six-coordinate MoO^{4+} complexes.[12] The compounds were formulated as MoO(cat)(Sap) derivatives containing the tridentate Schiff base ligand, Sap^{2-} = *N*-salicylidene-2-aminophenolate, and one of three bidentate catecholate ligands (Cat^{2-}, $Naphcat^{2-}$ or $DTBcat^{2-}$)[13] coordinated to MoO^{4+}. The unusual six-coordinate structure produced a dramatic electrochemical result; the normally irreversible reduction of the seven-coordinate MoO^{4+} center[8-11] became reversible when the coordination number was reduced to six.[12] It therefore became of interest to determine the structure of one compound of this class to establish the molecular structural basis for the change in electrochemical behavior. The present paper describes the synthesis and characterization of the three MoO(cat)(Sap) complexes and reports the X-ray crystal structure of the MoO(Naphcat)(Sap) derivative, which confirms the proposed six-coordinate geometry. To our knowledge this structural type has not been reported previously for MoO^{4+} complexes.[14]

Experimental Section

Materials and Methods. All syntheses were carried out under an argon atmosphere by using standard Schlenk tube techniques and degassed

---

(1) (a) Florida Atlantic University. Present address: Department of Chemistry, Pan American University, Edinburgh, TX 78539. (b) Indiana University-Purdue University at Indianapolis. (c) Notre Dame University.

(2) (a) Garner, C. D.; Bristow, S. In *Molybdenum Enzymes*; Spiro, T. G., Ed.; Wiley: New York, 1985; Chapter 7. (b) *Molybdenum and Molybdenum-Containing Enzymes*; Coughlan, M. P., Ed.; Pergamon: New York, 1980. (c) Burgmayer, S. J. N.; Stiefel, E. I. *J. Chem. Educ.* **1985**, *62*, 943.

(3) (a) Pope, M. T. *Heteropoly and Isopoly Oxomolybdates*; Springer-Verlag: West Berlin, 1983; and references therein. (b) Mitchell, P. C. H.; Sykes, A. G., Eds.; *Proceedings of the Climax Fifth International Conference on the Chemistry and Uses of Molybdenum*; Polyhedron Symposia-in-Print, Number 2; Pergamon: New York, 1986; pp 103-296.

(4) (a) Ricard, L.; Weiss, R. *Inorg. Nucl. Chem. Lett.* **1974**, *10*, 217. (b) Dirand, J.; Ricard, L.; Weiss, R. *Inorg. Nucl. Chem. Lett.* **1975**, *11*, 661. (c) Dirand, J.; Ricard, L.; Weiss, R. *Transition Met. Chem. (Weinheim, Ger.)* **1976**, *1*, 2. (d) Dirand, J.; Ricard, L.; Weiss, R. *J. Chem. Soc., Dalton Trans.* **1976**, 278.

(5) Liebeskind, L. S.; Sharpless, K. B.; Wilson, R. D.; Ibers, J. A. *J. Am. Chem. Soc.* **1978**, *100*, 7061.

(6) (a) Newton, W. E.; Bravard, D. C.; McDonald, J. W. *Inorg. Nucl. Chem. Lett.* **1975**, *11*, 553. (b) Chen, G. J.-J.; McDonald, J. W.; Newton, W. E. *Inorg. Chim. Acta* **1980**, *41*, 49. (c) Newton, W. E.; McDonald, J. W.; Corbin, J. L.; Ricard, L.; Weiss, R. *Inorg. Chem.* **1980**, *19*, 1997. (d) Marabella, C. P.; Enemark, J. H.; Newton, W. E.; McDonald, J. W. *Inorg. Chem.* **1982**, *21*, 623.

(7) Wieghardt, K.; Holzbach, W.; Hofer, E.; Weiss, J. *Inorg. Chem.* **1981**, *20*, 343.

(8) Bristow, S.; Enemark, J. H.; Garner, C. D.; Minelli, M.; Morris, G. A.; Ortega, R. B. *Inorg. Chem.* **1985**, *24*, 4070.

(9) Ghosh, P.; Bandyopadhyay, P.; Chakravorty, A. *J. Chem. Soc., Dalton Trans.* **1983**, 401.

(10) (a) Bradbury, J. R.; Schultz, F. A. *Inorg. Chem.* **1986**, *25*, 4416. (b) Gheller, S. F.; Bradbury, J. R.; Pabon de Majid, L.; Newton, W. E.; Schultz, F. A. *Inorg. Chem.* **1988**, *27*, 359.

(11) (a) Bradbury, J. R.; Schultz, F. A. *Inorg. Chem.* **1986**, *25*, 4408. (b) Schultz, F. A. *J. Electroanal. Chem. Interfacial Electrochem.* **1986**, *213*, 167.

(12) Mondal, J. U.; Schultz, F. A., submitted for publication in *Inorg. Chim. Acta*.

(13) The catecholate ligands and their abbreviations are as follows: Cat^{2-} = catecholate, $DTBcat^{2-}$ = 3,5-di-*tert*-butylcatecholate, and $Naphcat^{2-}$ = naphthalene-2,3-diolate; cat^{2-} is used as a general abbreviation for catecholate.

(14) Possible exceptions include the following. (a) The catecholate-bridged dimer, $[MoO(DTBcat)_2]_2$: Buchanan, R. M.; Pierpont, C. G. *Inorg. Chem.* **1979**, *18*, 1616. (b) The proposed solution monomer, $MoO(DTBcat)_2$(solvent): Wilshire, J. P.; Leon, L.; Bosserman, P.; Sawyer, D. T. In *Molybdenum Chemistry of Biological Significance*; Newton, W. E., Otsuka, S., Eds.; Plenum: New York, 1980; pp 327-344. (c) The set of six-coordinate complexes formally related to *cis*-dioxomolybdenum(VI) in which one oxo ligand is replaced by a multiply bonded nitrogen donor: Chatt, J.; Crichton, B. A. L.; Dilworth, J. R.; Dahlstrom, P.; Zubieta, J. A. *J. Chem. Soc., Dalton Trans.* **1982**, 1041 and references therein.

0020-1669/88/1327-3950$01.50/0

solvents. Chloroform was distilled from P_4O_{10} and ethanol from magnesium ethoxide before use in synthetic procedures. 2,3-Dihydroxynaphthalene was recrystallized from benzene, 3,5-di-*tert*-butylcatechol was recrystallized from heptane, and catechol was used as received from Aldrich. The complex $MoO_2(acac)_2$[15] ($acac^-$ = acetylacetonate) and the ligand H_2Sap[16] were prepared by the literature method indicated. The acetonitrile used in electrochemical experiments was Burdick & Jackson distilled-in-glass solvent and was stored over dried molecular sieves. Tetra-*n*-butylammonium hexafluorophosphate ($(TBA)PF_6$) supporting electrolyte (Southwestern Analytical Chemicals) was vacuum dried before use.

Elemental analyses for carbon, hydrogen, and nitrogen were performed by Galbraith Laboratories, Inc. (Knoxville, TN). FT/IR spectra were recorded in KBr pellets on a Nicolet 5DXB spectrometer. UV-vis spectra were recorded in CH_3CN by using a Perkin-Elmer Model 552 spectrometer. Electron-impact-ionization mass spectra of thermally volatilized samples were obtained by the direct-insertion probe technique on a DuPont 21-492B spectrometer. An ionization voltage of 70 eV, an accelerating voltage of 1836 V, and probe and source temperatures of 230–250 and 310 °C, respectively, were used in these experiments. The ^{95}Mo NMR spectrum of MoO(Naphcat)(Sap) was recorded at 32.6 MHz on a Bruker AM500 spectrometer at the University of Arizona. The chemical shift is referenced to external sodium molybdate as described previously.[17] Electrochemical measurements were carried out in 0.1 M $(TBA)PF_6/CH_3CN$ on a BAS-100A electrochemical analyzer. The working and reference electrodes were a 0.02 cm^2 Pt disk and an aqueous Ag/AgCl half-cell, respectively. Potentials are reported versus the $E^{0\prime}$ of the ferrocene/ferrocenium couple.

Synthesis of Compounds. $[MoO_2(Sap)]_2$. This dimeric Mo(VI) complex was prepared by the following method, which is similar to that of Rajan and Chakravorty.[18] First, 2.10 g (10.0 mmol) of H_2Sap dissolved in 60 mL of hot ethanol was added to 3.20 g (10.0 mmol) of $MoO_2(acac)_2$ dissolved in 40 mL of hot ethanol. The solution was refluxed with stirring for 1 h, during which time a yellow precipitate of $MoO_2(Sap)(EtOH)$ formed.[17] This solid was collected by filtration, washed with ethanol, and converted to $[MoO_2(Sap)]_2$ by heating at 100 °C under vacuum. The conversion is accompanied by a change in color from yellow to light brown.

MoO(Cat)(Sap). A 0.5-g (0.74-mmol) sample of $[MoO_2(Sap)]_2$ and 0.17 g (1.50 mmol) of H_2Cat were refluxed with stirring in 40 mL of chloroform for 1.5 h under an atmosphere of argon. The solution was filtered hot, and 40 mL of dry heptane was added to the top of the filtrate. The solution was allowed to stand overnight. A dark-colored crystalline material was collected by filtration, washed several times with heptane, and dried unver vacuum. Yield: 72%.

MoO(Naphcat)(Sap) and MoO(DTBcat)(Sap). These compounds were synthesized by the method given for MoO(Cat)(Sap) except that a mole ratio of $[MoO_2(Sap)]_2$ to catechol of 1:3 was used in each case and the reaction mixture was refluxed for 24 h. The yield was >70% in both cases.

Crystal Structure Determination. A dark purple crystal of MoO(Naphcat)(Sap), an elongated hexagonal prism with approximate dimensions of 0.65 × 0.30 × 0.30 mm, was selected from the preparation described above and mounted on a glass fiber with the long axis roughly parallel to the ϕ axis. Preliminary crystallographic analysis was carried out on an Enraf-Nonius CAD4 diffractometer, which revealed a monoclinic crystal system, approximate lattice constants, and systematic absences uniquely consistent with the space group $P2_1/n$, the nonstandard setting of $P2_1/c$. The crystal was transferred to a Nicolet $P\bar{1}$ diffractometer for final cell constant determination and intensity data collection. All measurements were made with graphite-monochromated Mo Kα radiation (λ = 0.71073 Å). Final cell constants came from a least-squares refinement of the setting angles of 60 reflections collected at $\pm 2\theta$ and with $22 < 2\theta < 30°$ given by the centering program of the diffractometer. Final values are a = 9.961 (3) Å, b = 10.109 (2) Å, c = 38.929 (9) Å, β = 92.45 (2)°, and V = 3916.4 Å^3. For $Z = 8$ (a cell content of $8MoO_5NC_{23}H_{15}$), the calculated density is 1.63 g/cm^3; the observed density (flotation in aqueous ZnI_2) was 1.64 g/cm^3.

Intensity data collection was performed by "wandering" ω scans to a 2θ limit of 54.9°. Four representative standards were measured every 50 reflections during the course of data collection and declined by 1.6% over the 122 h required for data collection. A total of 18989 reflections were measured and averaged; 5863 averaged data had $F_o^2 > 3\sigma(F_o^2)$ and were considered observed (merging R = 3.8% on F_o). The data were not corrected for the small crystal decomposition or for absorption effects (μ = 0.687 mm^{-1}).

The structure was solved by the heavy-atom method. A Patterson calculation provided the coordinates of the two crystallographic unique molybdenum atoms; the remaining atoms were located in subsequent DIRDIF or difference Fourier runs.[19] After several cycles of full-matrix least-squares refinement, it became apparent that the C(17)–N link in one of the two independent molecules (B) of MoO(Naphcat)(Sap) was disordered. This disorder was modeled by the use of two separate atomic positions for each atom of the bridge with atomic occupancies of 0.60 and 0.40 (unprimed and primed atoms, respectively). The analogous link in molecule A is possibly also disordered since the anisotropic temperature factors of these two atoms appear to be somewhat larger than normal. Difference Fourier maps also suggested the presence of possible hydrogen atom positions. These hydrogen atom positions were idealized (C–H = 0.95 Å) and included as fixed contributors in all subsequent cycles of least-squares refinement. Final cycles of refinement utilized anisotropic temperature factors for all heavy atoms except for the disordered C(17), N pair of molecule B. The final values of the discrepancy indices are R_1 = 0.081 and R_2 = 0.097 with the error of fit = 2.07. A final difference Fourier map had five peaks with heights of 2.1–2.3 e/Å^3 that were all within 1.0 Å of a Mo atom; all other peaks were less than 1.0 e/Å^3. Final values of atomic coordinates of the two independent molecules of MoO(Naphcat)(Sap) are given in Table I; the anisotropic thermal parameters are reported in Table SI of the supplemenary material. Final values of the fixed hydrogen atoms coordinates are given in Table SII.

Results and Discussion

Synthesis and Characterization. We initially sought to prepare the MoO(cat)(Sap) complexes by reacting $MoO_2(Sap)$ with the appropriate catechol

$$MoO_2(Sap) + H_2cat \rightarrow MoO(cat)(Sap) + H_2O \qquad (1)$$

Similar neutralization reactions have proved effective in converting six-coordinate $MoO_2(L)_2$ complexes to seven-coordinate $MoO(cat)(L)_2$ species when L = $Et_2NCS_2^-$,[10a] R_2NO^-,[10b] and $C_5H_{10}NO^-$.[8] However, when isolated from ethanol or other strong donor solvents $MoO_2(Sap)$ exists as a six-coordinate adduct, e.g. $MoO_2(Sap)(EtOH)$,[18,20] and in this form does not participate in reaction 1. Consequently, we converted $MoO_2(Sap)(EtOH)$ to $[MoO_2(Sap)]_2$ by heating under vacuum and reacted the dimeric product with catechol, 3,5-di-*tert*-butyl catechol, and 2,3-dihydroxynaphthalene in chloroform to give the desired MoO(cat)(Sap) complexes

$$[MoO_2(Sap)]_2 + 2H_2cat \rightarrow 2MoO(cat)(Sap) + 2H_2O \qquad (2)$$

The success of reaction 2 versus reaction 1 apparently results from weakening of one oxo bond per molybdenum in a dimeric structure such as

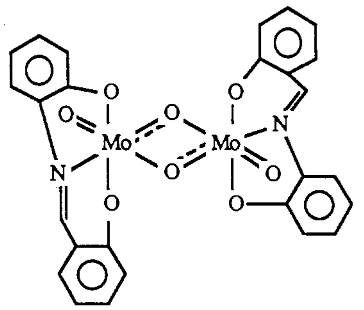

---

(15) Chen, G. J.-J.; McDonald, J. W.; Newton, W. E. *Inorg. Chem.* **1976**, *15*, 2612.

(16) Alyea, E. C.; Malek, A. *Can. J. Chem.* **1975**, *53*, 939.

(17) Young, C. G.; Roberts, S. A.; Ortega, R. B.; Enemark, J. H. *J. Am. Chem. Soc.* **1987**, *109*, 2938.

(18) Rajan, O. A.; Chakravorty, A. *Inorg. Chem.* **1981**, *20*, 660.

(19) DIRDIF: Beurskens, P. T.; Bosman, W. P.; Doesbury, H. M.; Gould, R. O.; van den Hark, Th. E. M.; Prick, P. A. J.; Noordik, J. H.; Stempel, M.; Smits, J. M. M. Technical Report 1984/1, Crystallography Laboratory: Toernooiveld, The Netherlands. Other programs used in this study included local modifications of Jacobson's ALLS, Zalkin's FORDAP, Busing and Levy's ORFFE, and Johnson's ORTEP2. Atomic form factors were from: Cromer, D. T.; Mann, J. B. *Acta Crystallogr., Sect. A* **1968**, *A24*, 321–323. Real and imaginary correlations for anomalous dispersion in the form factor of the molybdenum atoms were from: Cromer, D. T.; Liberman, D. J. *J. Chem. Phys.* **1970**, *53*, 1891–1898. Scattering factors for hydrogen were from: Stewart, R. F.; Davidson, E. R.; Simpson, W. T. *J. Chem. Phys.* **1965**, *42*, 3175–3187. All calculations were performed on a VAX 11/730.

(20) Topich, J. *Inorg. Chem.* **1981**, *20*, 3704.

Table I. Fractional Coordinates

atom	*x*	*y*	*z*
Mo(a)	0.84375 (6)	0.13380 (6)	0.069206 (13)
Mo(b)	0.28467 (6)	0.56109 (6)	0.207707 (12)
O(1a)	0.8307 (5)	0.3051 (5)	0.04594 (10)
O(2a)	0.8639 (5)	0.0842 (5)	0.02087 (11)
O(3a)	0.7717 (6)	0.2361 (6)	0.10588 (10)
O(4a)	0.8144 (6)	−0.0551 (6)	0.07441 (12)
O(5a)	1.0029 (5)	0.1248 (6)	0.08643 (13)
N(a)	0.6235 (8)	0.0895 (11)	0.06100 (17)
C(1a)	0.8490 (6)	0.3097 (7)	0.01180 (15)
C(2a)	0.8563 (7)	0.4217 (7)	−0.00760 (16)
C(3a)	0.8811 (7)	0.4103 (7)	−0.04272 (15)
C(4a)	0.8956 (6)	0.2833 (8)	−0.05745 (15)
C(5a)	0.8848 (8)	0.1695 (7)	−0.03708 (16)
C(6a)	0.8666 (7)	0.1819 (7)	−0.00244 (15)
C(7a)	0.8992 (8)	0.5220 (7)	−0.06421 (18)
C(8a)	0.9279 (9)	0.5073 (10)	−0.09782 (19)
C(9a)	0.9396 (9)	0.3848 (9)	−0.11190 (17)
C(10a)	0.9225 (8)	0.2755 (9)	−0.09261 (15)
C(11a)	0.6665 (8)	0.3174 (8)	0.10408 (16)
C(12a)	0.6649 (10)	0.4296 (10)	0.12383 (20)
C(13a)	0.5543 (11)	0.5097 (9)	0.12401 (24)
C(14a)	0.4476 (11)	0.4834 (11)	0.1042 (3)
C(15a)	0.4445 (9)	0.3705 (11)	0.08321 (26)
C(16a)	0.5550 (10)	0.2864 (9)	0.08367 (20)
C(17a)	0.5279 (11)	0.1581 (16)	0.06382 (25)
C(18a)	0.5995 (9)	−0.0520 (8)	0.04888 (18)
C(19a)	0.4864 (9)	−0.1153 (10)	0.03334 (21)
C(20a)	0.4927 (9)	−0.2511 (11)	0.02806 (22)
C(21a)	0.6121 (10)	−0.3201 (9)	0.03839 (23)
C(22a)	0.7201 (8)	−0.2556 (9)	0.05352 (20)
C(23a)	0.7139 (8)	−0.1207 (8)	0.05830 (17)
O(1b)	0.4256 (5)	0.4270 (5)	0.21034 (10)
O(2b)	0.2055 (5)	0.4181 (5)	0.18000 (11)
O(3b)	0.3940 (6)	0.6411 (5)	0.24528 (11)
O(4b)	0.1024 (6)	0.6255 (5)	0.20659 (14)
O(5b)	0.3320 (5)	0.6723 (5)	0.17877 (11)
N(b)	0.1678 (9)	0.4770 (9)	0.25136 (23)
N(b)′	0.2474 (13)	0.4807 (13)	0.26071 (29)
C(1b)	0.4082 (6)	0.3159 (7)	0.19077 (13)
C(2b)	0.4997 (7)	0.2187 (7)	0.18694 (16)
C(3b)	0.4694 (7)	0.1130 (7)	0.16352 (16)
C(4b)	0.3443 (7)	0.1121 (6)	0.14594 (14)
C(5b)	0.2506 (7)	0.2111 (7)	0.15119 (15)
C(6b)	0.2835 (6)	0.3105 (6)	0.17324 (14)
C(7b)	0.5581 (8)	0.0092 (8)	0.15766 (19)
C(8b)	0.5232 (10)	−0.0918 (8)	0.13508 (20)
C(9b)	0.4039 (9)	−0.0944 (8)	0.11842 (18)
C(10b)	0.3154 (8)	0.0045 (8)	0.12238 (16)
C(11b)	0.4313 (8)	0.5849 (7)	0.27458 (15)
C(12b)	0.5471 (8)	0.6349 (7)	0.29293 (17)
C(13b)	0.5844 (7)	0.5764 (9)	0.32349 (17)
C(14b)	0.5186 (10)	0.4709 (9)	0.33650 (18)
C(15b)	0.4036 (9)	0.4231 (8)	0.31938 (19)
C(16b)	0.3572 (7)	0.4825 (8)	0.28832 (17)
C(17b)	0.2246 (11)	0.4414 (11)	0.28063 (26)
C(17b)′	0.1271 (18)	0.4355 (18)	0.2706 (4)
C(18b)	0.0185 (7)	0.4727 (8)	0.24656 (20)
C(19b)	−0.0875 (10)	0.4078 (8)	0.26118 (19)
C(20b)	−0.2161 (10)	0.4313 (10)	0.24849 (25)
C(21b)	−0.2361 (9)	0.5212 (11)	0.22098 (24)
C(22b)	−0.1353 (8)	0.5862 (9)	0.20773 (19)
C(23b)	−0.0028 (8)	0.5605 (8)	0.21978 (18)

[a] The estimated standard deviations of the least significant digits are given in parentheses.

which would facilitate its replacement by catechol.

Analytical and spectroscopic data for the complexes are collected in Table II. The complexes exhibit a single strong infrared absorption at 930–939 cm^{-1}, which is characteristic of the Mo═O vibration in the MoO^{4+} group.[4-10] The possibility of geometrical isomerism (observed in the case of MoO(DTBcat)$(ONR_2)_2$[10b]) exists for the DTBcat derivative depending on the orientation of the unsymmetrically substituted catechol ligand with respect to the $[MoO(Sap)]^{2+}$ center. The IR spectrum of MoO(DTBcat)(Sap) exhibits only a single ν(Mo═O). Thus, either isomerism does not exist for this compound or the difference in interaction of the *tert*-butyl groups with the remainder of the molecule is insufficient to produce distinct Mo═O frequencies.

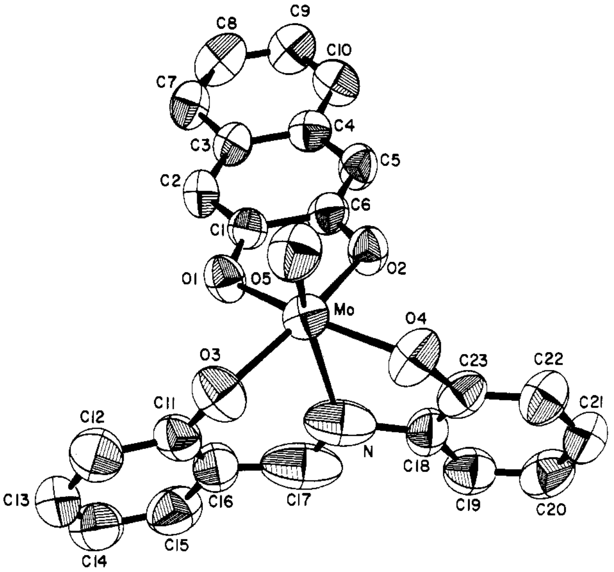

Figure 1. ORTEP drawing of molecule A. Atoms are contoured to enclose 50% of the electron density.

The MoO(cat)(Sap) complexes also exhibit an electronic absorption at 626–674 nm that is assigned to cat → Mo charge transfer. A similar transition is observed in MoO(cat)$(L)_2$ complexes with L = $Et_2NCS_2^-$,[10a] R_2NO^-,[10b] and $C_5H_{10}NO^-$.[8] Additional absorption bands observed at higher energies for the MoO(cat)(Sap) complexes (Table II) are assigned to inter- and intraligand transitions.

The ^{95}Mo NMR spectrum of MoO(Naphcat)(Sap) in $CDCl_3$ exhibits a single resonance at +385 ppm with respect to external molybdate with a line width of 160 Hz. This chemical shift is significantly more positive than values observed for seven-coordinate monooxomolybdenum(VI) (−55 to +5 ppm)[8,10b,21] and six-coordinate dioxomolybdenum(VI) (−219 to +58 ppm)[21] complexes with nitrogen and oxygen donors. The shift of +385 ppm lies at the low end of the range of values observed for $[Mo(V)_2O_4]^{2+}$ complexes. While this result could suggest a Mo(V) center tightly coupled to an organic radical anion, the structure of MoO(Naphcat)(Sap) (vide infra) indicates that Naphcat is coordinated as catecholate rather than semiquinone. It is tempting also to rationalize the chemical shift in terms of the unusual coordination number of MoO^{4+}. However, the ^{51}V shieldings of VO^{3+} complexes having CN = 4, 6, and 7 are not significantly influenced by changes in this parameter.[22] The shielding of heavy nuclei depends almost exclusively on the localized paramagnetic term,[21] which varies inversely as the energy of the lowest lying electronic transition. Since cat → Mo charge transfer occurs at significantly longer wavelengths for MoO(cat)(Sap) complexes compared with MoO(cat)$(ONR_2)_2$[10b] and MoO(cat)$(S_2CNEt_2)_2$,[10a] this factor probably is responsible for the unusually positive chemical shift of MoO(Naphcat)(Sap).

Molecular Structure. The molecular structures of the two independent molecules of MoO(Naphcat)(Sap) are displayed in Figures 1 (molecule A) and 2 (molecule B) which have been drawn with the same relative molecular orientation. Detailed values of bond distances and bond angles are given in Tables III and IV. The agreement in structural parameters between the two crystallographically independent molecules is quite satisfactory; averaged values for the two molecules will generally be quoted. This internal agreement suggests that the disorder in molecule B is

---

(21) Minelli, M.; Enemark, J. H.; Brownlee, R. C.; O'Connor, M. J.; Wedd, A. G. *Coord. Chem. Rev.* **1985**, *68*, 169.

(22) Rehder, D.; Weidemann, C.; Duch, A.; Priebsch, W. *Inorg. Chem.* **1988**, *27*, 584.

Table II. Analytical and Spectroscopic Data for MoO(cat)(Sap) Complexes

	anal. % calcd (% found)			IR $\nu_{Mo=O}$,	UV/vis[a]	MS	
compd	C	H	N	cm^{-1}	λ_{max}, nm (ϵ, M^{-1} cm^{-1})	fragment	m/e[b] (%)
MoO(Cat)(Sap)	52.91 (53.11)	3.04 (3.30)	22.25 (21.95)	939	628 (3010)	$[MoO(Cat)(Sap)]^+$	431 (100)
					453 (8170)	$[MoO_2(Sap)]^+$	339 (44)
					350 (21 800)	$[MoO(Sap)]^+$	323 (88)
					266 (18 900)		
MoO(Naphcat)(Sap)	57.39 (55.55)	3.14 (3.67)	19.93 (17.82)	936	626 (sh)	$[MoO(Naphcat)(Sap)]^+$	481 (74)
					458 (8140)	$[MoO_2(Sap)]^+$	339 (100)
					353 (22 900)	$[MoO(Sap)]^+$	323 (89)
					268 sh		
MoO(DTBcat)(Sap)	59.67 (59.28)	5.38 (5.44)	17.65 (17.25)	930	674 (3490)	$[MoO(DTBcat)(Sap)]^+$	543 (78)
					455 (9160)	$[MoO(DTBcat)\text{-}CH_3(Sap)]^+$	528 (100)
					352 (24 200)	$[MoO_2(Sap)]^+$	339 (48)
					274 (18 900)	$[MoO(Sap)]^+$	323 (25)

[a] CH_3CN. [b] m/e corresponding to ^{96}Mo isotope.

Table III. Bond Distances (Å) for MoO(Naphcat)(Sap)

	molecule A	molecule B		molecule A	molecule B
Mo–O(1)	1.956 (5)	1.951 (5)	C(14)–C(15)	1.404 (14)	1.387 (12)
Mo–O(2)	1.966 (4)	1.950 (4)	C(15)–C(16)	1.391 (13)	1.410 (10)
Mo–O(3)	1.926 (5)	1.961 (5)	C(16)–C(11)	1.374 (11)	1.391 (11)
Mo–O(4)	1.943 (6)	1.927 (6)	C(23)–C(18)	1.371 (12)	1.378 (11)
Mo–O(5)	1.697 (5)	1.673 (5)	C(18)–C(19)	1.409 (12)	1.385 (12)
Mo–N	2.248 (8)	2.266 (9)	C(19)–C(20)	1.389 (14)	1.375 (13)
Mo–N′		2.263 (12)	C(20)–C(21)	1.422 (13)	1.412 (14)
O(1)–C(1)	1.350 (7)	1.364 (8)	C(21)–C(22)	1.369 (12)	1.323 (13)
O(2)–C(6)	1.342 (8)	1.369 (8)	C(22)–C(23)	1.378 (11)	1.405 (10)
O(3)–C(11)	1.332 (9)	1.314 (8)	C(3)–C(7)	1.421 (10)	1.397 (10)
O(4)–C(23)	1.335 (9)	1.357 (10)	C(7)–C(8)	1.359 (11)	1.381 (11)
C(1)–C(2)	1.365 (9)	1.354 (9)	C(8)–C(9)	1.361 (13)	1.330 (12)
C(2)–C(3)	1.404 (9)	1.429 (9)	C(9)–C(10)	1.351 (11)	1.346 (11)
C(3)–C(4)	1.417 (10)	1.396 (9)	C(10)–C(4)	1.408 (8)	1.444 (9)
C(4)–C(5)	1.404 (10)	1.390 (9)	C(16)–C(17)	1.528 (17)	1.405 (12)
C(5)–C(6)	1.374 (8)	1.353 (8)	C(16)–N′		1.500 (13)
C(6)–C(1)	1.420 (10)	1.392 (8)	C(17)–N	1.187 (13)	1.301 (13)
C(11)–C(12)	1.370 (12)	1.423 (10)	C(17′)–N′		1.353 (22)
C(12)–C(13)	1.367 (13)	1.366 (10)	C(18)–N	1.522 (12)	1.492 (11)
C(13)–C(14)	1.313 (14)	1.361 (12)	C(18)–C(17′)		1.449 (18)

reasonably well described by the model defined in the Experimental Section.

The structure determination clearly shows the six-coordinate nature of the complexes and confirms the validity of the synthetic strategy as way of preparing six-coordinate Mo(VI) species containing only one multiply bound oxo ligand. A significant difference relative to the structure of seven-coordinate MoO^{4+} complexes is the orientation of the catecholate ligand. In MoO(Cat)$(ONC_5H_{11})_2$,[8] the catecholate ligand occupies one equatorial position and the axial site trans to terminal oxo. In MoO(Naphcat)(Sap), the catecholate oxygens are found at equatorial positions exclusively. As is readily seen from Figures 1 and 2, the four phenoxy oxygen atoms of MoO(Naphcat)(Sap) can be regarded as defining an equatorial plane with the oxo ligand and the nitrogen donor of the Sap ligand defining the two trans vertices of the octahedron. This four-oxygen-atom equatorial plane is almost exact in both molecules; the molybdenum(VI) atom is displaced 0.28–0.29 Å from this plane toward the oxo ligand. The O–Mo–N bond angle is about 20° less than the ideal value of 180°; presumably, the major reason for this deviation is the constraint imposed on the nitrogen donor position by the coordination of the tridentate Schiff base (the Sap ligand). The two phenolate rings in either of the two Sap ligands are not coplanar, but rather form dihedral angles of 23.5° (molecule A) or 29.5° (molecule B). The plane of the catecholate ligand is essentially coplanar with the O_4 equatorial plane in both molecules. Thus, the overall disposition of the ligands is consistent with that generally observed,[23] namely that the weakest π-donor is trans to the terminal oxo ligand.

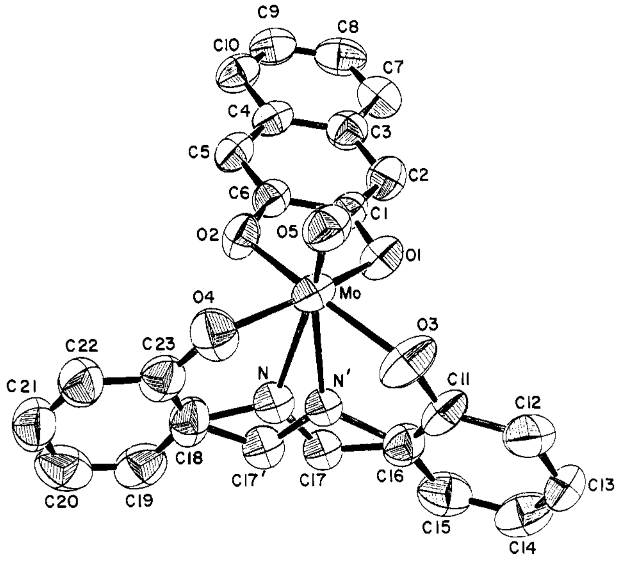

Figure 2. ORTEP drawing of molecule B.

The average oxo–Mo(VI) bond distance in the two independent molecules of MoO(Naphcat)(Sap) is 1.685 (17) Å; a value well within the range observed for a number of seven-coordinate MoO^{4+} complexes.[5,6d,7,24] The average phenoxy–Mo(VI) distance is 1.948

---

(23) Butcher, R. J.; Penfold, B. R.; Sinn, E. *J. Chem. Soc., Dalton Trans.* **1979**, 688.

(24) (a) Wieghardt, K.; Hofer, E.; Holzbach, W.; Nuber, B.; Weiss, J. *Inorg. Chem.* **1980**, *19*, 2927. (b) Schlemper, E. O.; Schrauzer, G. N.; Hughes, L. A. *Polyhedron* **1984**, *3*, 377. (c) Wieghardt, K.; Holzbach, W.; Hofer, E.; Weiss, J. *Chem. Ber.* **1981**, *114*, 2700. (d) Le Capentier, J.-M.; Schlupp, R.; Weiss, R. *Acta Crystallogr., Sect. B* **1972**, *B28*, 1278.

Table IV. Bond Angles (deg) for MoO(Naphcat)(Sap)

	molecule A	molecule B
O(1)–Mo–O(2)	77.9 (2)	77.7 (2)
O(1)–Mo–O(3)	81.3 (2)	82.6 (2)
O(1)–Mo–O(4)	155.6 (2)	155.6 (2)
O(1)–Mo–O(5)	105.8 (2)	106.2 (2)
O(1)–Mo–N	93.8 (3)	95.3 (3)
O(1)–Mo–N′		81.3 (4)
O(2)–Mo–O(3)	154.5 (2)	156.5 (2)
O(2)–Mo–O(4)	82.6 (2)	83.1 (2)
O(2)–Mo–O(5)	103.5 (2)	104.2 (2)
O(2)–Mo–N	87.3 (2)	85.9 (3)
O(2)–Mo–N′		99.2 (3)
O(3)–Mo–O(4)	112.8 (2)	111.7 (2)
O(3)–Mo–O(5)	96.1 (2)	93.5 (2)
O(3)–Mo–N	79.6 (3)	83.2 (3)
O(3)–Mo–N′		64.9 (4)
O(4)–Mo–O(5)	92.8 (3)	92.9 (2)
O(4)–Mo–N	70.7 (3)	68.3 (3)
O(4)–Mo–N′		87.2 (4)
O(5)–Mo–N	159.2 (3)	157.7 (3)
O(5)–Mo–N′		156.5 (4)
N–Mo–N′		21.9 (3)
Mo–O(1)–C(1)	118.5 (4)	117.9 (4)
Mo–O(2)–C(6)	117.7 (4)	118.4 (4)
Mo–O(3)–C(11)	127.6 (4)	126.6 (4)
Mo–O(4)–C(23)	123.5 (5)	124.8 (5)
Mo–N–C(17)	130.8 (11)	122.9 (8)
Mo–N–C(18)	111.8 (6)	117.3 (6)
Mo–N′–C(16)		120.4 (7)
Mo–N′–C(17′)		124.1 (10)
O(1)–C(1)–C(2)	125.9 (6)	126.1 (6)
O(1)–C(1)–C(6)	112.2 (6)	113.3 (6)
C(19)–C(18)–C(23)	121.7 (8)	121.3 (7)
C(11)–C(16)–C(17)	127.4 (9)	130.4 (7)
C(11)–C(16)–N′		96.7 (7)
C(15)–C(16)–C(17)	112.9 (9)	109.1 (8)
C(15)–C(16)–N′		144.2 (8)
C(23)–C(18)–N	106.0 (8)	101.3 (7)
C(23)–C(18)–C(17′)		137.8 (10)
C(19)–C(18)–N	132.2 (9)	137.3 (8)
O(2)–C(6)–C(5)	127.2 (7)	126.0 (5)
O(2)–C(6)–C(1)	113.5 (5)	112.1 (5)
C(6)–C(1)–C(2)	121.9 (5)	120.6 (6)
C(1)–C(2)–C(3)	119.1 (6)	119.2 (6)
C(2)–C(3)–C(4)	119.6 (6)	118.5 (6)
C(3)–C(4)–C(5)	120.2 (5)	121.0 (6)
C(4)–C(5)–C(6)	119.8 (7)	118.8 (6)
C(5)–C(6)–C(1)	119.3 (7)	121.8 (6)
C(2)–C(3)–C(7)	122.7 (6)	123.2 (6)
C(5)–C(4)–C(10)	121.7 (7)	121.3 (6)
C(4)–C(3)–C(7)	117.6 (6)	118.2 (6)
C(3)–C(7)–C(8)	121.2 (7)	121.0 (7)
C(7)–C(8)–C(9)	120.8 (8)	121.3 (8)
C(8)–C(9)–C(10)	120.4 (7)	120.3 (7)
C(9)–C(10)–C(4)	121.9 (8)	121.3 (7)
C(10)–C(4)–C(3)	118.1 (7)	117.7 (6)
O(3)–C(11)–C(12)	120.6 (7)	118.4 (7)
O(3)–C(11)–C(16)	120.3 (7)	121.4 (6)
O(4)–C(23)–C(22)	121.2 (8)	120.9 (7)
O(4)–C(23)–C(18)	118.2 (8)	120.1 (7)
C(16)–C(11)–C(12)	119.0 (8)	120.2 (6)
C(11)–C(12)–C(13)	121.4 (9)	117.9 (7)
C(12)–C(13)–C(14)	120.6 (9)	123.1 (7)
C(13)–C(14)–C(15)	120.3 (10)	119.7 (7)
C(14)–C(15)–C(16)	119.5 (10)	119.8 (7)
C(15)–C(16)–C(11)	119.2 (9)	119.1 (6)
C(18)–C(23)–C(22)	120.4 (8)	118.9 (8)
C(23)–C(22)–C(21)	119.4 (8)	119.7 (8)
C(22)–C(21)–C(20)	121.3 (9)	122.0 (8)
C(21)–C(20)–C(19)	119.0 (8)	118.8 (9)
C(20)–C(19)–C(18)	118.2 (9)	119.1 (8)
C(19)–C(18)–C(17′)		100.0 (10)
N–C(18)–C(17′)		38.1 (7)
N′–C(16)–C(17)		36.3 (6)
C(16)–C(17)–N	114.6 (11)	118.3 (10)
C(17)–N–C(18)	117.5 (11)	119.7 (9)
C(18)–C(17′)–N′		112.1 (14)
C(16)–N′–C(17′)		115.4 (11)

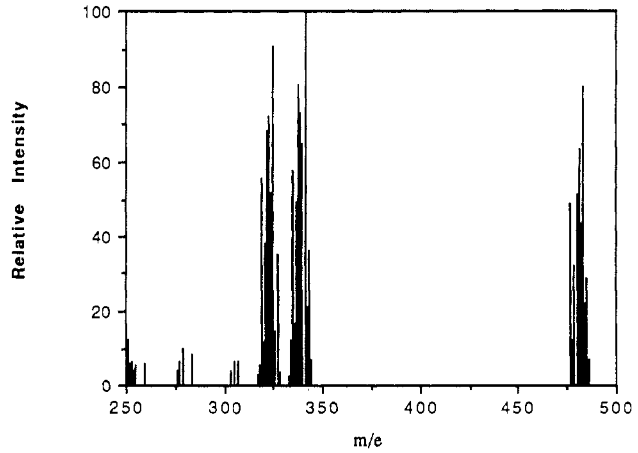

Figure 3. Positive ion EI mass spectrum of MoO(Naphcat)(Sap) from *m/e* ≥250.

(15) Å, a value appropriate for the anionic nature of these ligands. Bonds trans to terminal oxo ligands are expected to display lengthening owing to a structural trans effect. However, the observed average Mo–N bond distance of 2.259 (10) Å appears to be somewhat shorter than expected based on other structures. Mo–N bond distances cis to terminal Mo–O groups range[6d,24a,b,25] from 2.058 to 2.199 Å. Values for Mo–N bond distances trans to terminal oxo ligands range[26] from 2.237 to 2.486 Å. This sample includes two Schiff base nitrogen distances of 2.237 and 2.304 Å; distances to aromatic nitrogen donors are in the range 2.30–2.35 Å. We thus conclude that steric constraints of the

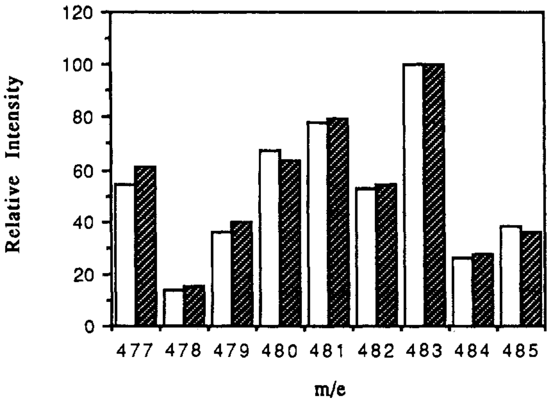

Figure 4. Observed (shaded) and calculated (open) isotope distribution patterns of $[MoO(Naphcat)(Sap)]^+$.

---

(25) (a) Gullotti, M.; Pasini, A.; Zanderighi, G. M.; Ciani, G.; Sironi, A. *J. Chem. Soc., Dalton Trans.* **1981**, 902. (b) Attanasio, D.; Dessy, G.; Fares, V. *Inorg. Chim. Acta* **1985**, *104*, 99.

(26) (a) Yamanouchi, K.; Enemark, J. H. *Inorg. Chem.* **1979**, *18*, 1626. (b) Buchanan, I.; Minelli, M.; Ashby, M. T.; King, T. J.; Enemark, J. H.; Garner, C. D. *Ibid.* **1984**, *23*, 495. (c) Bruce, A.; Corbin, J. L.; Dahlstrom, P. L.; Hyde, J. R.; Minelli, M.; Stiefel, E. I.; Spence, J. T.; Zubieta, J. *Ibid.* **1982**, *21*, 917. (d) Subramanian, P.; Spence, J. T.; Ortega, R.; Enemark, J. H. *Ibid.* **1984**, *23*, 2564. (e) Berg, J. M.; Spira, D. J.; Hodgson, K. O.; Bruce, A.; Miller, K. F.; Corbin, J. L.; Stiefel, E. I. *Ibid.* 3412. (f) Berg, J. M.; Holm, R. H. *J. Am. Chem. Soc.* **1985**, *107*, 917. (g) Schrauzer, G. N.; Hughes, L. A.; Schlemper, E. O.; Ross, F.; Ross, D. *Organometallics* **1983**, *2*, 1163. (h) Schrauzer, G. N.; Hughes, L. A.; Strampach, N.; Ross, F.; Ross, D.; Schlemper, E. O. *Ibid.* 481. (i) Viossat, B.; Rodier, N. *Acta Crystallogr., Sect. B* **1979**, *B35*, 2715.

Table V. Electrochemical Data for Reduction of MoO(cat)(Sap) Complexes[a]

	first wave			second wave		
compd	$E^{0\prime}$, V (ΔE_p, mV)	$i_{pc}/v^{1/2}AC$,[b] μA s$^{1/2}$ V$^{-1/2}$ cm^{-2} mM^{-1}	i_{pa}/i_{pc}[c]	E_{pc},[d] V	$E_{pc} - E_{p/2}$,[d] mV	$i_{pc}/v^{1/2}AC$,[b] μA s$^{1/2}$ V$^{-1/2}$ cm^{-2} mM^{-1}
MoO(Cat)(Sap)	-0.583 (69)	990	0.98	-1.793	83	770
MoO(Naphcat)(Sap)	-0.514 (82)	820	0.96	-1.652	70	600
MoO(DTBcat)(Sap)	-0.691 (68)	780	0.97	-1.887	114	560

[a] Recorded for ca. 1 mM complexes in 0.1 M (TBA)PF_6/CH_3CN at Pt electrode over a sweep rate range of 0.02–0.2 V s^{-1}. [b] Evaluated from slope of i_{pc} vs $v^{1/2}$ plot. [c] Measured after sweeping through both reduction waves. [d] Value at v = 0.2 V s^{-1}.

tridentate ligand may lead to a small shortening of the Mo–N bond.

The bond distances in the Schiff base and catecholate ligands are unexceptional for the dianionic forms of these ligands. Of particular note is the fact that the average C–C (1.389 (27) Å in molecule A, 1.383 (35) Å in molecule B) and C–O (1.346 (4) Å in molecule A, 1.366 (2) Å in molecule B) distances in Naphcat are fully in accord with coordination of this ligand in the catecholate rather than the semiquinone form.[27]

Mass Spectrometry. Figure 3 shows the positive ion EI mass spectrum of MoO(Naphcat)(Sap). Each complex exhibits a well-defined spectrum of this type containing a significant molecular ion peak. Data from the *m/e* range above 200 and peak assignments are contained in Table II. Each of these peaks exhibits an isotope distribution pattern characteristic of molybdenum. Agreement between observed and calculated distributions for the [MoO(Naphcat)(Sap)]$^+$ fragment is illustrated in Figure 4.

In addition to the molecular ion peak, all complexes yield fragments at *m/e* 339 and 323. The DTBcat spectrum also contains an M – 15 fragment that corresponds to loss of CH_3 from [MoO(DTBcat)(Sap)]$^+$. The common *m/e* 323 fragment corresponds to loss of the catecholate ligand from [MoO(cat)(Sap)]$^+$, as exemplified for cat^{2-} = $C_6H_4O_2{}^{2-}$ in eq 3. If initial electron

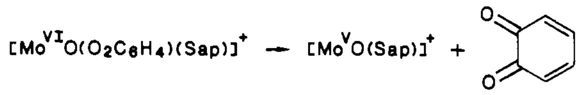

(3)

abstraction occurs from the coordinated catechol ligand as it does in the solution electrochemistry of MoO(cat)$(S_2CNEt_2)_2$[10a] and MoO(cat)$(ONR_2)_2$,[10b] then eq 3 is an internal redox process in which the metal center is reduced from Mo(VI) to Mo(V) and semiquinone is released as quinone. The *m/e* 339 peak corresponds to a second process in which the [MoO$_2$(Sap)]$^+$ fragment is generated by cleavage of a C–O bond and release of coordinated semiquinone as a phenoxy radical

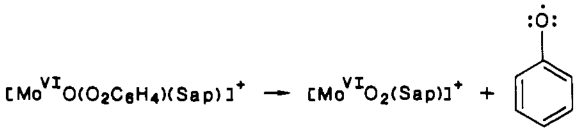

(4)

The charge on the [MoO$_2$(Sap)]$^+$ fragment suggests that the coordinated Sap ligand has been oxidized by one electron in the process. Ligand fragmentation is not unusual in the mass spectrometry of coordination compounds,[28] and eq 4 is almost certainly driven by formation of $MoO_2{}^{2+}$, which reflects the strong oxygen affinity of the electropositive MoO^{4+} center. However, eq 4 contrasts with the FAB mass spectrometry of $MoO_2(S_2CNEt_2)_2$[29] where the molecular ion experiences *loss* of O in preference to a chelate ligand.

Electrochemistry. Figure 5 illustrates the cyclic voltammetric reduction of MoO(Cat)(Sap) in acetonitrile. The behavior shown there is typical of all three MoO(cat)(Sap) complexes. Figure 5a typifies the response at sweep rates above 0.1 V s^{-1}; Figure 5b describes the response at slower sweep rates. Electrochemical data are presented in Table V.

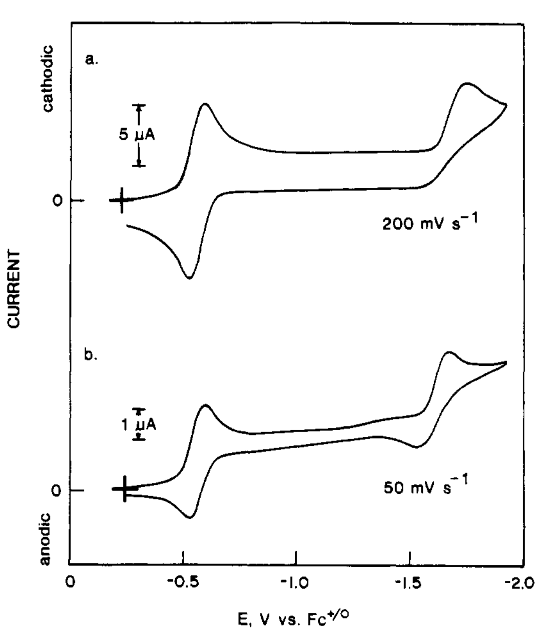

Figure 5. Cyclic voltammetry of 1 mM MoO(Cat)(Sap) in 0.1 M Bu_4NPF_6/CH_3CN: (a) 200 mV s^{-1}; (b) 50 mV s^{-1}.

At sweep rates above 0.1 V s^{-1}, MoO(cat)(Sap) reduction proceeds by reversible one-electron transfer at -0.5 to -0.7 V vs. Fc$^{+/0}$ followed by irreversible one-electron transfer at -1.65 to -1.9 V.

$$[\mathrm{Mo^{VI}O(cat)(Sap)}] + e^- \rightleftharpoons [\mathrm{Mo^{V}O(cat)(Sap)}]^- \quad (5)$$

$$[\mathrm{Mo^{V}O(cat)(Sap)}]^- + e^- \rightarrow [\mathrm{Mo^{IV}O(cat)(Sap)}]^{2-} \quad (6)$$

The diffusion-controlled one-electron character of reactions 5 and 6 is established by the fact that their voltammetric peak currents vary linearly with the square root of sweep rate and that the parameters derived from this response (Table V) are consistent with one-electron transfer in acetonitrile.[11a,30] Reaction 5 is both chemically and electrochemically reversible. The separation between its cathodic and anodic peak potentials is approximately equal to the value we observe under experimental conditions for a reversible one-electron transfer without compensation of solution resistance (ΔE_p = 65 mV, ferrocene oxidation), and i_{pa}/i_{pc} = 1. Controlled-potential coulometric reduction of MoO(DTBcat)(Sap) at -0.9 V vs. Fc$^{+/0}$ consumes 0.99 faraday/mol of Mo and produces a solution exhibiting an oxidative voltammogram with the same $i_p/v^{1/2}AC$ and $E^{0\prime}$ values as the MoO(DTBcat)(Sap)reduction wave.[31]

---

(27) (a) Buchanan, R. M.; Pierpont, C. G. *J. Am. Chem. Soc.* **1980**, *102*, 4951. (b) Pierpont, C. G.; Buchanan, R. M.; *Coord. Chem. Rev.* **1981**, *38*, 45.

(28) Litzow, M. R.; Spalding, T. R. *Mass Spectrometry of Inorganic and Organometallic Compounds*. Elsevier: Amsterdam: 1973, Chapter 11.

(29) Cerny, R. L.; Sullivan, B. P.; Bursey, M. M.; Meyer, T. J. *Anal. Chem.* **1983**, *55*, 1954.

(30) The current parameter of reaction 6 is 20–30% smaller than that of reaction 5. The difference is attributed to the irreversible character of the second reduction, which causes an increase in width and decrease in height of its voltammetric peak.

(31) Coulometric reduction of MoO(Cat)(Sap) at -0.8 V and of MoO(Naphcat)(Sap) at -0.7 V gives 0.75 and 0.74 faraday/mol of Mo, respectively. The reduced solutions exhibit waves for [MoO(cat)(Sap)]$^-$ oxidation at the appropriate potentials, but the current parameters are only 50–70% of the original values. Since the Cat and Naphcat complexes exhibit reversible behavior on the time scale of cyclic voltammetry, we presume that chemical reactions occurring during the lengthier coulometry experiments consume a fraction of the initial reactant and result in a smaller accumulation of charge.

Scheme I

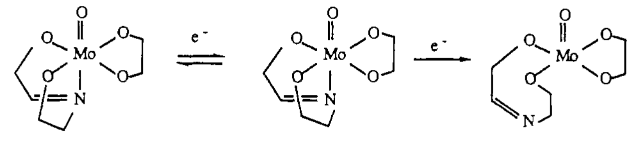

The reversible $Mo^{VI/V}$ electrochemistry exhibited by these six-coordinate MoO^{4+} complexes contrasts dramatically with the behavior of this functional group in a seven-coordinate environment.[12] Irreversible electrochemistry at seven-coordinate MoO^{4+} centers results from the fact that the four Mo d_{xy} orbital lobes that become singly occupied upon reduction to Mo(V) experience unfavorable interactions with the five equatorial bonds present in the pentagonal-bipyramidal geometry and initiate metal–ligand bond cleavage reactions during charge transfer. Preparation and structural characterization of six-coordinate MoO(cat)(Sap) complexes demonstrates that when only four bonds are present in the equatorial plane, these unfavorable interactions are absent and reversible one-electron electrochemistry prevails. The six-coordinate distorted-octahedral geometry of MoO(Naphcat)(Sap) is characteristic also of monooxomolybdenum(V) (MoO^{3+}) complexes,[2a,32] consequently we expect that Mo(VI) to Mo(V) reduction of MoO(cat)(Sap) proceeds with minimal structural change as shown in the first step of Scheme I.

Figure 5a shows that the second reduction of MoO(Cat)(Sap) (eq 6) is irreversible at a sweep rate of 0.2 V s^{-1}. The voltammetric peak widths ($E_p - E_{p/2} = 70$–110 mV) and shifts in voltammetric peak potential with sweep rate ($\Delta E_p/\Delta(\log v) = 55$–70 mV) are consistent with slow heterogeneous charge transfer.[33] Thus, we conclude that a change in structure accompanies reduction of Mo(V) to Mo(IV). Since monooxomolybdenum(IV) most commonly exists in a five-coordinate square-pyramidal environment[34] and structural constraints involving the Mo–N bond in MoO(Naphcat)(Sap) have been noted earlier, a probable structural change is displacement of the Schiff base N atom trans to terminal oxo as shown in the second half of Scheme I.

Figure 5 further shows that the second MoO(Cat)(Sap) reduction wave experiences a transition from irreversible to quasireversible behavior as the sweep rate is reduced from 200 to 50 mV s^{-1}. All three MoO(cat)(Sap) complexes exhibit a similar anodic peak at sweep rates below 0.1 Vs^{-1}. This unusual observation suggests that a slow chemical reaction takes place following irreversible Mo(V) reduction, which facilitates Mo(IV) oxidation on the positive sweep. A possible explanation of this behavior is reattachment of the Schiff base N atom to Mo (possibly in a different configuration) via a process conceptually similar to the base-on/base-off reactions associated with the cobalt-centered electrochemistry of vitamin B-12 derivatives.[35] A considerable activation energy barrier must be associated with this process because it occurs at a relatively slow rate and results in large separations between the anodic and cathodic peak potentials. ($\Delta E_p = 150$–200 mV at $v = 0.05$ V s^{-1}).

Acknowledgment. We wish to acknowledge financial support from the National Science Foundation (Grant No. CHE-87-18013, F.A.S.) and the National Institutes of Health (Grant No. GM-38401-16, W.R.S.). We thank Dr. J. W. Louda (Florida Atlantic University) and Professor John H. Enemark and M. LeBarre (University of Arizona) for obtaining and providing assistance in interpreting mass and ^{95}Mo NMR spectra, respectively.

Supplementary Material Available: Table SI, anisotropic thermal parameters for MoO(Naphcat)(Sap), and Table SII, fixed hydrogen atom coordinates (3 pages); a listing of observed and calculated structure factor amplitudes (×10) (20 pages). Ordering information is given on any current masthead page.

---

(32) Cleland, W. E., Jr.; Barnhart, K. M.; Yamanouchi, K.; Collison, D.; Mabbs, F. E.; Ortega, R. G.; Enemark, J. H. *Inorg. Chem.* **1987**, *26*, 1017.

(33) Nicholson, R. S.; Shain, I. *Anal. Chem.* **1964**, *36*, 706.

(34) Stiefel, E. I. *Prog. Inorg. Chem.* **1977**, *22*, 1.

(35) Lexa, D.; Saveant, J. M. *Acc. Chem. Res.* **1983**, *16*, 235.

Contribution from the Laboratoire de Chimie des Organométalliques associé au CNRS (UA 415),
Université de Rennes I, 35042 Rennes Cedex, France

Synthesis and Proton NMR Studies of the Electronic Structure of Ferric Phosphine Porphyrin Complexes

G. Simonneaux* and P. Sodano

Received April 14, 1988

The preparation and spectral properties of low-spin ferric phosphine complexes of a series of synthetic and natural porphyrins have been reported. The proton NMR spectra of $Fe(TPP)(PMe_3)_2ClO_4$ and $Fe(TPP)(PMe_3)(1\text{-MeIm})ClO_4$ have been analyzed. The axial ligand hyperfine shifts have been separated into their dipolar and contact contributions by using both the dominant dipolar shifts for certain porphyrin positions and the magnetic anisotropy data derived from low-temperature ESR spectra. The contact shifts are shown to arise primarily from iron → phosphine π^* charge transfer. The trimethylphosphine H peak is shown to shift characteristically upfield on going from $[Fe(TPP)(PMe_3)_2]^+$ to $[Fe(TPP)(PMe_3)(1\text{-MeIm})]^+$, confirming that this resonance may serve as a new probe for hemoproteins.

Recent investigations in this laboratory have focused on phosphorus-ligated hemoprotein complexes.[1-3] ^{1}H and ^{31}P NMR techniques have been used to probe the size of the ligand-binding pocket in hemoglobins (Hb) and myoglobin (Mb). The ligand used is a phosphine, PMe_3, which is small enough to complex Hb. In particular, we reported new and definite evidence on direct observation of intermediate ligation states of hemoglobin based on ^{31}P NMR spectra of partially ligated $HbPMe_3$.[4]

Phosphines serve also as useful probes of ferric hemoprotein electronic and molecular structures in part through generation

---

(1) Bondon, A.; Petrinko, P.; Sodano, P.; Simonneaux, G. *Biochim. Biophys. Acta* **1986**, *872*, 163.

(2) Bondon, A.; Sodano, P.; Simonneaux, G.; Craescu, C. T. *Biochim. Biophys. Acta* **1987**, *914*, 289.

(3) Simonneaux, G.; Bondon, A.; Sodano, P. *Inorg. Chem.* **1987**, *26*, 3636.

(4) Simonneaux, G.; Bondon, A.; Brunel, C.; Sodano, P. *J. Am. Chem. Soc.*, in press.